

# Finite Element Modelling Versus Reality for Birch Chairs

Stig-Inge Gustafsson,  
IKP/Wood Science and Technology  
Institute of Technology, S 581 83 Linköping, Sweden

## Abstract

When chairs and other furniture are designed the work is mostly founded on handicraft experience. Calculations based on solid mechanics theory are almost never used in order to find out optimal solutions for different wood members, or the structure as a whole. We have therefore studied a simple chair, made of birch, where the emphasis is laid on its ability to carry different loads. Using the method of finite elements we have predicted the strain and stress at different points on the chair structure. Further, we have manufactured the chair and exposed it to the same load pattern as used in the finite element calculations. The strain has been monitored and compared to the calculated value at the points of most interest. The result shows that part of the calculations corresponded fairly well with the monitored values but also that much work still remains in order to totally predict the accurate structural behaviour for such a simple frame as a chair. Probably, some of the discrepancies depend on the wood material which exhibits so different response for stress in different directions.

## INTRODUCTION

In recent years, more interest has been shown for wood as a material. This, because of the advantages from an environmental view. Wood is a renewable resource and further, there is no problem when e. g. furniture is taken out of service life. It is even possible to use it as fuel in the form of biomass. Aesthetic reasons many times also speak for wood. However, there is a debate about using woods from the rain forests and therefore, wood species which grow in our own country would be perfect as raw material. In Sweden, much effort has been laid upon research about wood of spruce and fir which are the main species for our export. Less emphasis has been put on our broad leaved types, such as birch, alder, maple and so forth. Sweden also acts as an undeveloped country when one considers that almost all our wood is exported as sawed lumber. If more of the wood could be utilised and converted to finished products this could have an important effect on our trade balance and budget deficit.

Furniture design in Sweden, as well as in other countries, rests upon tradition and handicraft experience. It is nothing wrong with that but, by the use of modern computers and sophisticated mathematical models, it should be possible to find new ways to design chairs as well as other furniture in order to utilise the

material much better than before. However, the scientific research in this field does not seem to have the highest priority. We have only found four groups in the world dealing with this subject. First we have Eckelman and a few others in the U.S.A. In e.g. Reference [1] the author, as early as 1966, shows how a chair works as a mechanical structure and how it carries the loads exerted by ordinary people. He also calculates the moment at different spots in the structure for various locations of a stretcher. His work has after this continued and in Reference [2] the knowledge in this field is presented in a book containing about 400 pages. Other contributors are the authors to Reference [3] where case furniture, such as cabinets, are studied. Chairs and structural mechanics have also been of interest in Poland. In Reference [4] the authors shows the result from calculations on cabinets but they have also published papers about chairs. The most interesting from our point of view seems unfortunately only to be available in Polish. In Japan they have studied furniture joints in more detail, see e.g. Reference [5]. Hitherto, our own contributions, dealing with structural mechanics and furniture, is limited to Reference number [6] where we optimised the location of a chair stretcher and in Reference [7] examined the stability problems on compressed members in a chair. The studied structure in Reference [6] as well as the result are shown in Figure 1.

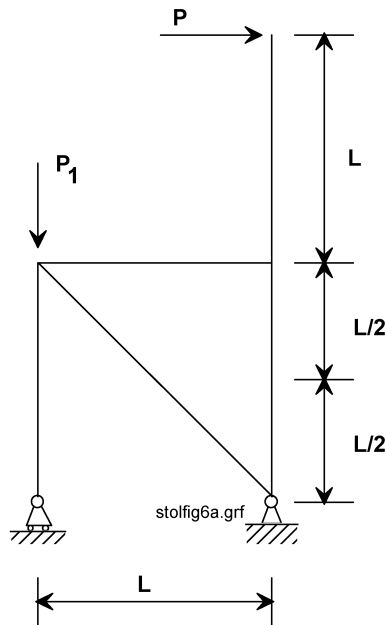


Figure 1: Optimal location of a chair stretcher in order to minimise the moment in the joint where the seat meets the back rail, [6].

The main result of our calculations in Reference [6] was that the stretcher should be located as low as possible on the back rail and as high as possible

at the front rail. This, of course, only as long as the loads do not change. These findings encouraged us to actually manufacture the chair as designed in Figure 1, and after this to use it for experiments. The interesting thing to study is if these more complicated methods, such as the finite element method, are applicable for such a complicated material as wood. The chair is manufactured in birch and we have therefore started by some minor materials investigations for this wood species.

## TESTING OF BIRCH AS A MATERIAL

In e. g. Reference [8] or [9] some values could be found for birch as a construction material. For a start, Young's modulus are shown to be about 166,700 kp/cm<sup>2</sup> or 16,670 MPa in the direction along the grain, 630 MPa in radial direction and 1,130 MPa in the tangential direction. The rigidity modulus, G, are for the directions xz, yz and xy 1,200, 190 and 930 MPa where x is the radial, y is the longitudinal and z is the tangential direction, see Reference [8] page 295. It is obvious that the direction of the load is essential to the resulting stress and strain. These values show how wood acts in the elastic region. If the load is increased, the material comes into the plasticity region and no linear relationship between strain and stress is found. Further, it is also of interest to study what actually happens when the load is increased to the level of rupture because it is possible to design furniture to that point or at least immediately below it. It is not a catastrophe if a chair breaks and hence it is possible to use much higher design stresses than are used for buildings etc. In Figure 2 a tensile test is shown for birch.

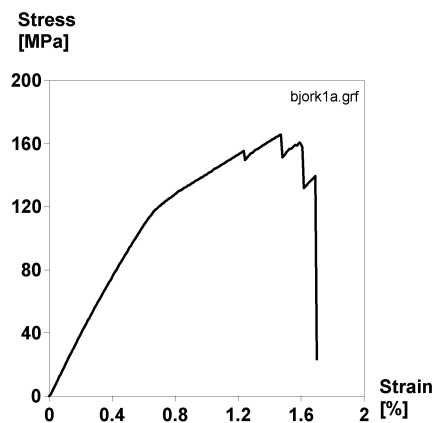


Figure 2: Tensile test for birch

From Figure 2 it is obvious that the strength of rupture is about 165 MPa. This is more than was shown in Reference [9], page 164, which was 134 MPa. Obvious is also that there are two distinct moduli of elasticity, one below the

marked knee, i. e. 18,200 and one above which was calculated to 6,450 MPa. Another phenomenon is the fact that birch does not break at one specific stress. When the stress in Figure 2 was about 160 MPa you could hear some fibres in the material break, but almost instantly, others came into rescue. A significant extra strain could therefore be introduced without a total collapse in the material. We also want to mention some difficulty in applying the correct length of the wooden test specimens when the strain is to be calculated. Not always did they break at their thinnest part. Instead a long crack many times occurred which lead in under the grips of the tensile test apparatus. Using extensometers to a part solved this problem but they malfunctioned when the region of fibre breaking occurred. The resulting strain stress curves were then useless for scientific evaluations.

Problems also occurred when performing compression tests. We found it of great importance to choose short specimens with sufficient cross sectional area. Otherwise the material started to plasticise immediately because only a corner of the specimen was used for carrying all the load. In Figure 3 one of the compression tests is shown.

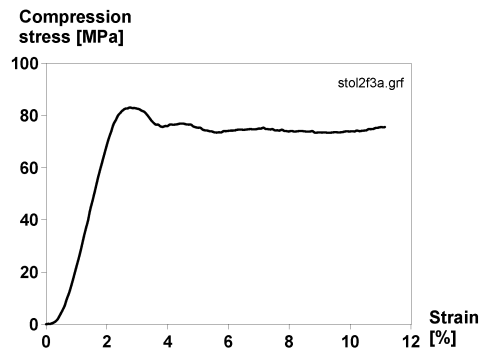


Figure 3: Compression test for birch

The compression Young's modulus was calculated to 4,700 MPa which is about one fourth of the tension modulus. The compression strength of rupture is about 82 MPa in Figure 3, which is about half the value of the applicable tension strength. It is also obvious that a load higher then the crushing strength does not lead to disaster. The wood specimen endures a lot of strain without breaking totally to pieces.

The fact that wood shows such a big difference between tensile and compression strength has implied the common use of bending strength as a value to be used in structural mechanics calculations. The standardised method assumes that the stress is linearly and symmetrically distributed over the cross section which cannot be valid for wood, where the behaviour differs so much between tension and compression, see [8] page 360 for more details. In Figure 4 a three point bending test is shown for birch.

Note that the bending stress is calculated as:

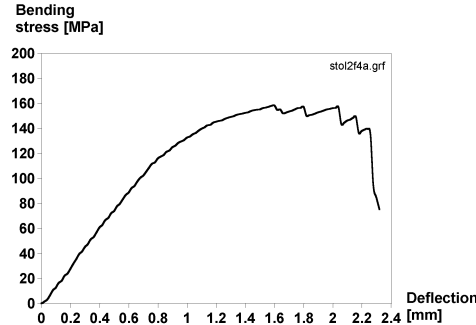


Figure 4: Stress-deflection curve for birch

$$\sigma = \frac{M \times z}{I} \quad \text{where} \quad M = \frac{P \times L}{4} \quad \text{and} \quad I = \frac{b \times h^3}{12}$$

$P$  shows the load in N,  $L$  the span and  $M$  the moment in the middle of the span.  $I$  is the moment of inertia,  $b$  the breadth and  $h$  the height of the rectangular test specimen. The curve seems to be perfectly linear up to a value of about 120 MPa and after this the specimen starts to plasticise. Of interest is also the fact that the beam did not break at a specific point. Some fibres seems to break at about 160 MPa and a deflection of 1.6 mm, but as found in the tension test others carry the load instead.

If the bending stress is reached, immediate disaster is therefore not inevitable. However, the construction can not carry such a load for longer periods of time. In the case of a chair the person sitting on it will of course rise when the wood starts to creak. The modulus of elasticity, MOE, see Reference [8] page 300, for a bending test is calculated as:

$$E_b = \frac{P \times L^3}{4 \times y \times w \times h^3}$$

where  $P$  equals the breaking load,  $L$  the length of the specimen span,  $y$  the deflection,  $w$  the width and  $h$  the depth. In our case, this calculation results in a MOE of 13,450 MPa. All our wood specimens had moisture contents of about 6 %.

## FINITE ELEMENT CALCULATIONS

In Reference [7] we have shown that the method of displacement could be used when calculating internal stress and strain for members in an indetermined frame. In such a frame, these values could not be calculated without considering the rotations and displacements of the frame. It is not possible to show the method in its entirety, not even in Reference [7], because of the limited number of pages and therefore the interested reader is referred to Reference [10] for all

details. However, the displacement method uses the fact that by introducing rotations and displacements it is possible to elaborate the stiffness matrix of the indetermined frame. In Figure 5 a simplified frame is shown of the members of interest in the chair.

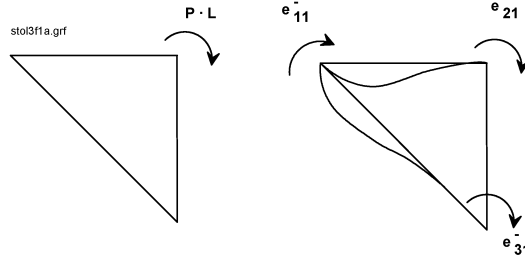


Figure 5: Back rail, seat rail and stretcher in the simplified frame

In Figure 5 the back rail, which is a statically determined part, has been replaced by a moment  $P \times L$ . The front leg is likewise statically determined and therefore not used for finding the matrix. The indetermined frame that is left must be analysed by use of the deformations in the frame. Therefore, the cross sectional areas must be known for the different members. In Reference [7] we used a stretcher of 0.005 times 0.02 m which was probably too weak because of stability problems. In our experiment chair the stretcher is stronger, with a cross sectional area of 0.01 times 0.02 m. The back rail is 0.01 times 0.03 m and the same is valid for the seat rail. The displacement method now tells us that the moments acting on the frame by the introduction of the rotation in the left part of the frame is:

$$e_{11}^- = \frac{4EI_1}{L} + \frac{4EI_2}{L \times 2^{0.5}}$$

$$e_{21}^- = \frac{2EI_1}{L}$$

$$e_{31}^- = \frac{2EI_2}{L \times 2^{0.5}}$$

where  $I_1$  equals the moment of inertia for the seat rail and  $I_2$  the same value for the stretcher. The moment of inertia for the seat rail equals  $\frac{0.02 \times 0.03^3}{12}$  while the stretcher has a value of  $\frac{0.01 \times 0.02^3}{12}$ , or  $2.25 \times 10^{-8}$  and  $6.66 \times 10^{-9}$  respectively. The stretcher therefore has a moment of inertia that is one third of the one for the seat rail and hence they, below, are set to I and 0.3 I. Using the same method for the other six matrix elements results in the equation:

$$\begin{pmatrix} 4.94 & 2.0 & 0.47 \\ 2.0 & 8.0 & 2.0 \\ 0.47 & 2.0 & 4.94 \end{pmatrix} \times \frac{EI}{L} \times \begin{pmatrix} q_1 \\ q_2 \\ q_3 \end{pmatrix} = \begin{pmatrix} 0 \\ P \times L \\ 0 \end{pmatrix}$$

Solving this small system of equations results in  $q_1 = q_3 = -0.0567$  and,  $q_2 = +0.1533 \frac{PL^2}{EI}$ . We must also find the moments and internal forces, and from Reference [7] they are found as:

$$M_{12} = 4 \times 0.0567 \times \frac{PL^2}{EI} \times \frac{EI}{L} - 2 \times 0.1533 \times \frac{PL^2}{EI} \times \frac{EI}{L} = -0.0798PL$$

$$M_{21} = 2 \times 0.0567 \times \frac{PL^2}{EI} \times \frac{EI}{L} - 4 \times 0.1533 \times \frac{PL^2}{EI} \times \frac{EI}{L} = -0.4998PL$$

$$M_{23} = 4 \times 0.1533 \times \frac{PL^2}{EI} \times \frac{EI}{L} - 2 \times 0.0567 \times \frac{PL^2}{EI} \times \frac{EI}{L} = +0.4998PL$$

$$M_{32} = 2 \times 0.1533 \times \frac{PL^2}{EI} \times \frac{EI}{L} - 4 \times 0.0567 \times \frac{PL^2}{EI} \times \frac{EI}{L} = +0.0798PL$$

$$M_{31} = -4 \times 0.0567 \times 2^{-0.5} \times 0.3^3 \times \frac{PL^2}{EI} \times \frac{EI}{L} - 2 \times 0.0567 \times 2^{-0.5} \times 0.3^3 \times \frac{PL^2}{EI} \times \frac{EI}{L} = -0.0794PL$$

$$M_{13} = -2 \times 0.0345 \times 2^{-0.5} \times 0.3^3 \times \frac{PL^2}{EI} \times \frac{EI}{L} - 4 \times 0.0345 \times 2^{-0.5} \times 0.3^3 \times \frac{PL^2}{EI} \times \frac{EI}{L} = -0.0794PL$$

Due to the convention of signs and by inserting  $P = 300$  N and  $L = 0.4$  m the following moments apply:

$$\begin{aligned} M_{12} &= 9.58\text{Nm (tension below)} & M_{21} &= 60.0\text{Nm (tension above)} \\ M_{23} &= 60.0\text{Nm (tension inside)} & M_{32} &= 9.58\text{Nm (tension outside)} \\ M_{31} &= 9.58\text{Nm (tension outside)} & M_{13} &= 9.58\text{Nm (tension inside)} \end{aligned}$$

It is now possible to calculate the internal forces only by use of the equations of static equilibrium and the result is that the stretcher has a shear force of 34 N while the axial compression force is 636 N. The seat rail shear force is at the same time 174 N and the axial tension force 463 N. The back rail is compressed by a force of 174 N while the shear force is of the same size.

## VERIFICATION OR NOT

The moments and forces in the frame have now been calculated. We have also monitored the strain on four different points in our first experimental chair by using strain gauges of the type HMB LY 120-10. The first two points are located on each side of the back rail just above the seat rail. The next two points are located on each side of the stretcher and at half its length, see Figure 6.

In Figure 6 the number and location of the monitoring devices are shown. Further, the forces that are applied on the chair are presented, where  $P$  is the load that has been varied in the experiment.  $P_1$  shows a load of about 600 N that is applied in the front because else the chair would turn over. The force  $P_3$  only shows a fixed stop at the floor or otherwise the chair would slip when  $P$  is applied. The monitored strain is shown in Table 1.

As seen in the table we only have loads up to 150 N. This is so because the joint between the seat and the rail broke when 200 N was charged. The

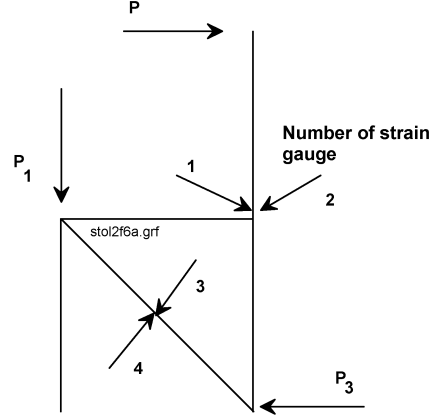


Figure 6: Location of the strain monitoring devices

Force [N]	Strain [ $\mu\text{m}/\text{m}$ ] for device nr			
	1	2	3	4
50	-456	+583	+32	+10
100	-808	+1001	+51	+32
150	-1095	+1562	+70	+63

Table 1: Monitored strain in  $\mu\text{m}/\text{m}$  for different loads  $P$  in N

dowel joint was not satisfactory manufactured. The negative values in the table show tension while positive values show compression. Firstly, note that only one of the points is tensed, i. e. number 1. Further, the strain on the tensed and the compressed side is not uniform. The compression strain is higher than the tension ditto. This may be the result of the different behaviour in tension and compression in wood where the two Young's moduli differ a lot. This also means that the unstressed layer, also called the neutral layer, is not located in the middle of the beam. If that layer had been exactly in the middle, the values for device number 1 would have been identical to the values for number 2, but with opposite sign.

The values in Table 1 shows the strain in  $\mu\text{m}/\text{m}$  or micro strain. The first two strain gauges are located 0.35 m from the force  $P$ . The moment for a test load of 50 N is therefore 17.5 Nm. The back rail is 0.02 times 0.03 m which results in a cross sectional area of 0.0006  $\text{m}^2$  and a moment of inertia,  $I$ , of  $4.5 \times 10^{-8} \text{ m}^4$ . The axial force is zero and therefore the stress,  $\sigma$ , could be calculated as:

$$\sigma = \frac{M \times z}{I} = \frac{17.5 \times 0.015}{4.5 \times 10^{-8}} = 5.83 \text{ MPa}$$

This stress must be divided by the value for the Young's modulus for birch,



18,200 MPa, as found above. The strain will therefore become 0.000320 or 320  $\mu\text{m}/\text{m}$ . The real strain, i.e. the one found in the experiment, is therefore somewhat larger than expected but its at least in the right magnitude. When 100 N is applied the strain must become 640  $\mu\text{m}/\text{m}$  and for 150 N it must be 960  $\mu\text{m}/\text{m}$  a value that corresponds at least to a certain amount with the one monitored for the tensed side.

Suppose we had chosen the lower value of the Young's moduli in Figure 2, i. e. 6,450 MPa, the first two values in Table 1 should be compared with 1,033  $\mu\text{m}/\text{m}$  which is not as close as before. Interesting to note is also that the increase in strain on the tensed side becomes smaller for larger loads but the opposite is valid on the compressed side. This should not happen according to Hooke's law.

In Table 1 the strain at the upper and lower part of the stretcher are shown. The moment in each end of the stretcher is  $0.0794 P \times L$  which for  $P = 50$  N and  $L = 0.4$  m will become 1.588 Nm. The left end is tensed on the upper side while the right side is tensed on the lower side. Exactly in the middle of the stretcher the moment therefore becomes zero, because the two moments are identical in size. The only forces acting here will hence, be axial forces and shear forces. When 50 N is applied the shear force could be calculated to 5.6 N and the axial force to 147 N. The stress here can be calculated as  $147 \text{ N} / 0.0006 \text{ m}^2 = 0.245$  MPa. Young's modulus in compression, see Figure 3, was calculated to 4,700 MPa and therefore the strain is calculated to 52  $\mu\text{m}/\text{m}$ , which is more than found in Table 1 but also of the right magnitude. More difficult to explain is the fact that the stretcher seems to be bent even if the theory says that this is not the fact. The values on the upper and lower sides of the stretcher seems, however, to get closer when the load is increased.

If the stretcher in fact is bent the moments of each side could not be equal in size. In order to study this, a second experiment has been elaborated see Figure 7 and Table 2.

Force [N]	Strain [ $\mu\text{m}/\text{m}$ ] for device nr				
	1	2	3	4	5
25	-155	-12	-11	-8	+41
50	-295	-26	-23	-11	+79
75	-405	-36	-34	-15	+104
100	-514	-45	-44	-12	+143
125	-641	-52	-51	-6	+165

Table 2: Monitored strain in  $\mu\text{m}/\text{m}$  for different loads  $P$  in N

The devices 1 and 2 are located under the seat rail as close to the respective corner as possible. Devices 3 and 5 are placed on the upper side of the stretcher while device number 4 is pasted as low as possible, at the inside of the back rail. From Table 2 it is shown that the strain is largest for device nr 1. This is logical because the moment is about six times higher here than at the other measuring points. The calculations showed that the moment is twice as large above the seat rail as it is under it. The strain should also reflect this. If experiment one and two are compared the strain above the rail was -456 and -808  $\mu\text{m}/\text{m}$  for 50 respective 100 N and -295 and -514  $\mu\text{m}/\text{m}$  for the device under the rail.

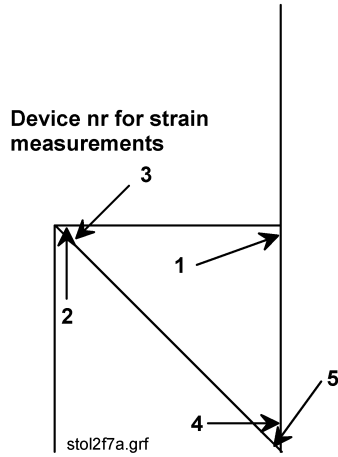


Figure 7: Location and number of strain gauge devices, experiment number two

There is therefore some discrepancy between the calculations and the monitored values. The real strain as monitored is also still higher than expected from the calculations above. For example, at a 100 N half the value of  $640 \mu\text{m/m}$  would have been perfect while  $514 \mu\text{m/m}$  instead was the fact.

Interesting to note is also the fact that the force - strain function follows an almost perfectly straight line, see Figure 8, which was predicted by the calculations.

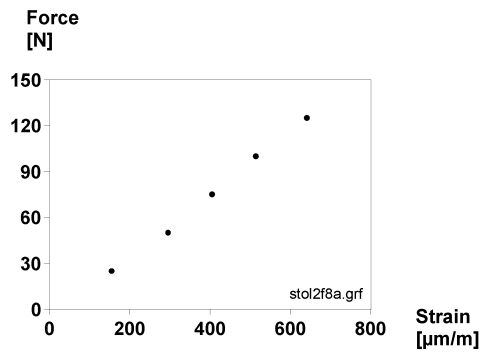


Figure 8: Force versus strain from device nr 1 in experiment 2.

This is not the fact for strain gauge nr 4 but, unfortunately, we do not know the reason for this. The strain values in point 2 and 4 differ a lot. The strain is about twice as large in point 2 compared to the one found in point 4. So do

the values differ for point 3 and 5. This could, however, be the result of the axial forces discussed above. For 50 N this axial force was calculated to 147 N resulting in a strain of  $52 \mu\text{m}/\text{m}$ . These 50 N also resulted in a moment of 1,6 Nm in each corner. The strain corresponding to that value is  $136 \mu\text{m}/\text{m}$ . The tensed side should therefore have a strain of  $136 - 52 = 84 \mu\text{m}/\text{m}$  while the compressed side should be  $136 + 52 = 188 \mu\text{m}/\text{m}$ . Instead the values are -23 and +79 respectively. However, it seems that the calculated moment in the corner is too large. The difference between the two monitored values is  $102 \mu\text{m}/\text{m}$  which is almost identical to the 104, i.e.  $52 + 52$ , which was calculated. The strain from bending only, should therefore be about  $28 \mu\text{m}/\text{m}$  or subsequently a moment of only 0.3 Nm.

The values for point 2 and 4 also show that they both are tensed. The calculations, however, showed that point 2 should have been tensed while point 4 would be compressed. Further, the back rail is exposed to an axial compression force which would have made the compression strain even higher. The reason for these discrepancies might be imperfect properties at the wood material or problems with the monitoring. Consider Figure 9.

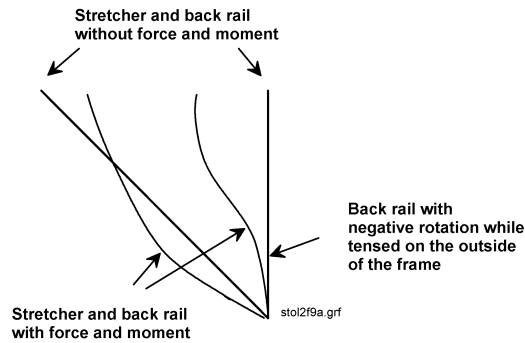


Figure 9: Exaggerated view of part of the chair frame

With the small rotations in our example, note that Figure 9 is greatly exaggerated, the tensed part of the back rail might be very short. From practical reasons it is not possible to monitor the strain at one specific point because the strain gauge is about two cm long. Further, it is not possible to place it absolutely in the corner where the tension must have its largest value.

## CONCLUSIONS

In this paper it is shown that calculated values, by use of a finite element method, many times have a fairly good correspondence with monitored values. However, problems also occur. Wood has different properties for tension and compression. This is shown by monitoring the strain at certain points of the chair frame. For some points the calculations implied that tension would prevail

but instead the experiments showed that this was not the fact. One explanation for this might be difficulties to monitor the strain at a very small point located in the corner of the frame. These values were also very small in magnitude and therefore a minute modification of the properties of the wooden material might have changed these monitored values. It also seems that more research is needed in order to understand how to modify the theory of strain and stress calculations especially for bent parts of a frame. This because the neutral layer moves when bending is intensified.

## ACKNOWLEDGEMENTS

The author wishes to thank NUTEK, the Swedish National Board for Industrial and Technical Development, for funding this research. Also many thanks to Bo Skoog at the Materials Testing Laboratory at the Department of Mechanical Engineering for all help with the testing equipment and Ljungstedt 's school for manufacturing the chairs.

## References

- [1] Eckelman C. A. A Look at the Strength Design of Furniture. *Forest Products Journal*, 16(3):21–24, 1966.
- [2] Eckelman C. A. Effective Principles of Product Engineering and Strength Design for Furniture Manufacturing. Technical report, Purdue University, West Lafayette, 1991.
- [3] Cai L. and Wang F. Influence of the Stiffness of Corner Joint on Case Furniture Deflection. *Holz als Roh- und Werkstoff*, 51:406–408, 1993.
- [4] Smardzewski J. and Dziegielewski S. Stability of Cabinet Furniture Backing Boards. *Wood Science Technology*, 28:35–44, 1993.
- [5] Wang S. Y. and Juang H. B. Structural Behaviour of Various Joints in Furniture Components Made of Softwood Laminated Veneer Lumber. *Mokuzai Gakkaishi*, 40(9):911–921, 1994.
- [6] Gustafsson S. I. Furniture Design by use of the Finite Element Method. *Holz als Roh- und Werkstoff*, 53(?):257–260, 1995.
- [7] Gustafsson S.-I. Stability Problems in Optimised Chairs. *Wood Science and Technology*, 30(?):339–345, 1996.
- [8] Kollmann F. and Côté W. *Principles of Wood Science and Technology, Volume I*. Springer-Verlag, 1984. ISBN 3-540-04297-0.
- [9] Tsuomis G. *Science and Technology of Wood*. Van Nostrand Reinhold, 1991. ISBN 0-442-23985-8.
- [10] Hsieh Y. *Elementary Theory of Structures*. Prentice Hall, 1970. ISBN 0-13-261512-6.